Journal of Information Systems Engineering and Management
2025, 10(15s)
e-ISSN: 2468-4376
https://www.jisem-journal.com/

Research Article

Integrating AHP, GIS, and TOPSIS, for Optimal Dam Site Selection: Leveraging Valley Derivation and Contour Line Analysis to Mitigate Flood Risks in Baghdad, Iraq

Suhailah Najm Rahim[1*], Barat Mojaradi[1*]
[1] Hossein Alizade[2]
, Muthanna Al-Shammari[3], Ahmed H. Shihab[4]

ARTICLE INFO

Received: 01 Dec 2024
Revised: 27 Jan 2025
Accepted: 05 Feb 2025

ABSTRACT

Assessing flood risk and identifying flood-prone areas are extremely important in scientific and engineering fields. Iraq faces significant challenges due to climate variability, experiencing hot and dry conditions in summer, water scarcity, cold and rainy winters, heavy rainfall that can lead to floods, and Water seepage into the ground. This article's significance extends beyond the accumulation of rainwater and floods during peak seasons; it also addresses the need to manage and mitigate floods in the event of the potential collapse of the Mosul Dam, which is currently at risk of failure. Additionally, the annual earthquakes along the Turkish-Iraqi border threaten dam infrastructure. This requires strong management strategies to reduce the severity and associated flood risks to choose the optimal dam building location. The study aims to organize water flow dynamics and develop, analyze, and evaluate the analytical hierarchy process (AHP) rooted in the theory of (multi-criteria decision-making (MCDM)). The paper integrates valley derivation and contour lines as core techniques within the GIS framework. This is not commonly found in most studies that use AHP and TOPSIS for dam site selection. Special importance is given to identifying hydrological features while considering the impacts of climate change. It combines these methods with six layers of GIS data (e.g., NDVI, NDWI, NDBI, NDMI), which provides a comprehensive hydrological and topographical analysis of flood-prone areas. Introduce weights to distance transformation in the AHP-TOPSIS workflow, offering a novel mathematical approach to decision-making in dam site selection. Four potential dam site options (C1, C2, C3, and C4) are evaluated through valley derivations and contour lines analysis, leading to the identification of three promising dams (A, B, and C). By comparing these, the most optimum dam can be determined. The study findings indicate that site C1 received the highest rating (P = 0.667) with a completion rate of 88.15%. "Dam A = region C1" The volume of dam A is 31 million cubic meters, a storage capacity of 28,177,200 cubic meters, a pixel area of 900, a total dam area of 775,000 square meters, and a height of 40 meters, making it the most suitable option among the alternatives.

Keywords: “Dam site selection”,” valley derivation "," contour lines "," Flood risk management "," GIS ", "AHP "," TOPSIS”, “Baghdad”

NOMENCLATURE

Abbreviation	Definition
GIS	Geographic Information Systems
LULC	land use and land cover
AHP	Analytic Hierarchy Process
MCDA	Multi-Criteria Design Analysis
TOPSIS	Technique for Order Preference by Similarity to Ideal Solution
NDVI	Normalized Difference Vegetation Index
NDBI	Normalized Difference Built-Up Index
NDWI	Normalized Difference Water Index
NDMI	Normalized Difference Moisture Index

INTRODUCTION

The global water resource crisis, aggravated by climate change, profoundly threatens human well-being, economic stability, and sustainable development. Shifts in precipitation patterns have intensified the frequency of extreme weather events, manifesting as floods and droughts, with severe repercussions for ecosystems, agriculture, and

infrastructure (Al-Ansari et al., 2014). Iraq, home to the historically vital Tigris and Euphrates River systems, faces a dual crisis: escalating water scarcity and heightened flood risks. These challenges are compounded by upstream water management practices, changing climatic conditions, and an aging infrastructure network (Mourad, 2023; Eklund et al., 2023). Floods rank among the most devastating natural disasters, with their frequency and intensity amplified by climate change and inefficient water management systems. The vulnerability of Iraq's critical infrastructure, particularly the Mosul Dam, underscores the severity of the risk. A potential failure of this dam would result in catastrophic downstream flooding, threatening densely populated urban centers (Eklund et al., 2023). Despite existing flood control measures, the limited capacity to manage extreme weather events highlights the pressing need for strategic interventions that balance the dual pressures of water scarcity and flood mitigation (Al-Ansari et al., 2014). Advances in Geographic Information Systems (GIS), remote sensing, and hydrological modeling offer transformative tools for flood risk management. These technologies enable precise identification of flood-prone areas, comprehensive assessment of flood susceptibility, and targeted mitigation strategies (Zahraa Al-Ali et al., 2022; Ahmed et al., 2021). The integration of GIS with hydrological models, such as HEC-RAS, has proven invaluable in simulating flood behavior, informing policy, and enhancing decision-making processes (Huali Chen et al., 2020). However, Iraq's water management systems face significant pressures. Limited channel capacities, coupled with aging and insufficient infrastructure, hinder effective flood control (Mourad, 2023). The growing unpredictability of rainfall patterns further exacerbates these vulnerabilities (Ahmed et al., 2021). Addressing these complex challenges demands a multi-faceted, data-driven approach that integrates advanced technologies and robust decision-making frameworks (Zahraa Al-Ali et al., 2022; Al-Ansari et al., 2014).

" This study proposes a novel methodology that integrates GIS, hydrological modeling, and innovative decision-making techniques to enhance flood risk management in Iraq. Building upon existing research, it incorporates valley derivation and contour analysis within the GIS-based Analytic Hierarchy Process (AHP), offering a unique hydrological and topographical perspective. Additionally, transforming weights into distances within the AHP-TOPSIS framework establishes a standardized and scalable approach to evaluating potential dam locations. Unlike previous studies, this methodology improves flood mitigation strategies and provides a transferable framework that can be adapted to other regions facing similar hydrological challenges. "

LITERATURE REVIEW

Scientists have employed various approaches to identify flood-prone areas. Anne Gacul (2022) utilized DEMATEL combined with sensitivity analyses to refine the accuracy of the Flood Hazard Index (FHI) and Flood Vulnerability Index (FVI). This methodology emphasized the importance of effective weight determination in improving the reliability of flood hazard assessments. Similarly, Zahraa Al-Ali et al. (2022) leveraged the Fuzzy Analytic Hierarchy Process (FAHP) integrated with GIS to conduct spatial evaluations of flood risk in Santa Fe, utilizing datasets sourced from governmental entities and online platforms. Their approach highlighted GIS's capability to manage spatial data for identifying and prioritizing flood risks. However, these studies relied on static datasets, underscoring the need for real-time data integration to improve the temporal accuracy of flood risk assessments. Remote sensing and GIS methodologies have been widely adopted to identify flood hazard zones. Ahmed et al. (2022) employed an integrated approach that combined GIS, remote sensing, and the Analytical Hierarchy Process (AHP) to delineate flood hazard zones, selecting nine parameters based on their relevance to flood prediction. Mitra et al. (2022) also utilized GIS and AHP to identify flood vulnerability and risk zones. Both studies underscored the utility of GIS in processing spatial data, yet neither incorporated socio-economic factors, which are essential for comprehensive risk evaluations, particularly in urban and densely populated areas. Hydrological and statistical modeling have further enhanced flood risk prediction capabilities. Abdelhafid Alaoui Fels et al. (2022) developed flood hazard index maps by applying probabilistic methods and hydrodynamic modeling, while Liu et al. (2021) focused on real-time flood prediction using distributed hydrological models. Liu's work introduced a composite warning index (CWI), which derived flash flood warning thresholds based on soil moisture, peak flow, and water levels. These contributions demonstrate the potential of hydrological models to improve flood prediction; however, their reliance on high-resolution datasets can limit their application in resource-constrained regions. Advanced computational techniques, including machine learning and artificial intelligence, have addressed some of the limitations of traditional methods. Pulvirenti et al. (2021) applied deep learning algorithms to process heterogeneous datasets, significantly improving flood extent mapping accuracy compared to conventional models. Similarly, Sadiq et al. (2022) combined machine learning with weighted overlay techniques in GIS to predict flash flood vulnerabilities. These approaches demonstrate the potential of big data and AI in overcoming the limitations of static models, though their scalability remains a challenge. Despite these advancements, significant gaps persist. Many models rely heavily on high-resolution spatial datasets, which may not be accessible in all regions, limiting their global applicability (Makkulawu et al., 2023). Additionally, the integration of socio-economic data into flood risk models remains underexplored, which hinders the development of holistic and inclusive flood mitigation strategies (Ma & Mostafavi, 2024).

This study aims to address these gaps by integrating GIS, AHP, and advanced computational tools to develop a comprehensive framework for flood risk assessment. By leveraging these methodologies, the research seeks to

identify optimal dam construction sites, thereby contributing to effective flood risk mitigation and resource management.

DESCRIPTION OF THE STUDY AREA

Baghdad, located in central Iraq and bordered by Salah al-Din, Diyala, Anbar, and Babylon, lies between latitudes 33°19'34" and 33°32'6" north and longitudes 25°16'44" and 44°42" east. Chosen as a case study for its unique geographic and climatic conditions, Baghdad experiences scorching, arid summers with temperatures reaching 40°C to 50°C (104°F to 122°F), occasionally exceeding 50°C during heatwaves. Winters are cold, averaging 0°C to 10°C (32°F to 50°F), with rainfall mainly occurring in this season. Central Iraq receives 100 to 200 mm of annual rainfall, while northern areas, such as Kurdish regions, receive higher amounts ranging from 400 to 600 mm annually (Awadh, 2024; Muslih & Abbas, 2024; Al-Khalidi et al., 2024; Nassif et al., 2024). Historical floods in Baghdad, notably the catastrophic events of 1954 and 1988, emphasized the city's vulnerability to hydrological extremes due to inadequate drainage capacity. The 2017 urban flooding further exposed deficiencies in the city's drainage systems (Mahdi, 2020; Al-Hussein, 2024). These incidents underscore the urgency of implementing effective water management measures, including dam construction, to mitigate future flood risks. The region's climatic fluctuations highlight the critical need for efficient water management strategies. With hot summers necessitating water storage for irrigation and winter rainfall increasing flood risks, the impact of global warming intensifies these challenges, straining Baghdad's infrastructure (Awadh, 2024; Muslih & Abbas, 2024). Studies in semi-arid regions have shown the effectiveness of using geographic and climatic data for site selection and flood risk management (Alrawi et al., 2021). As illustrated in Figure (1).

METHODOLOGY

BACKGROUND

Integration of AHP, TOPSIS, and GIS for Optimal Dam Region Selection. Refining the Analytic Hierarchy Process (AHP) methodology in decision-making enhances its scientific and engineering precision (Pathan et al., 2022). A central aspect of this refinement is the normalization of subjective weights assigned by decision-makers to ensure uniformity across the scale. Normalization techniques, such as vector normalization, have been shown to improve the consistency and reliability of AHP outcomes (Jozaghi et al., 2018). To further enhance objectivity, incorporating end-user evaluations as standardized weights is advocated. Additionally, introducing a convergence coefficient is crucial for establishing the hierarchy of alternatives. This coefficient plays a vital role in ranking choices by calculating their distances from both ideal and negative solutions, effectively translating weights into measurable distances (Rane et al., 2023). By adopting this approach, decision-makers gain access to a richer dataset, enabling more accurate and informed decisions. Building on these methodological improvements, this study emphasizes applying valley derivations and contour lines to identify optimal sites for dam construction. Integrating spatial analyses within a Geographic Information System (GIS) framework aims to mitigate flooding risks effectively. Combining AHP with the Technique for Order Preference by Similarity to the Ideal Solution (TOPSIS) within this framework offers a comprehensive solution for optimal dam site selection (Pathan et al., 2022, Rane et al., 2023). The integration of TOPSIS with valley derivations and contour lines facilitates the identification of multiple prospective dam sites. These sites are subsequently analyzed and compared to determine the most suitable location, based on a thorough evaluation of spatial patterns and interdependencies (Makkulawu et al., 2023). While promising, this approach requires robust spatial data, advanced computational tools, and skilled technical expertise to ensure its effectiveness and applicability. Future studies should validate the methodology through real-world case studies and address potential scalability challenges to broaden its use across diverse decision-making scenarios (Makkulawu et al., 2023, Rane et al., 2023). By addressing these considerations, the refined AHP methodology, integrated with TOPSIS and GIS, holds significant potential for improving decision-making accuracy in complex engineering projects such as dam Region selection. As Figure 2.

HYPOTHESES

1. Four regions, identified through weight-to-distance conversion and spatial analysis, are hypothesized to exhibit significant variations in suitability for dam construction based on hydrological, topographical, and geospatial criteria.
2. Six selected factors are analyzed and classified using GIS, which is hypothesized to yield spatial patterns optimized for flood risk mitigation and dam site selection.
3. Areas with pronounced valley features and specific contour patterns are hypothesized to correspond to natural water flow pathways and high flood risk zones.
4. The spatial alignment of topographical valley characteristics and contour patterns is hypothesized to significantly influence the identification of suitable dam sites for flood prevention.

5. Leveraging GIS techniques, including valley derivation and contour analysis, is hypothesized to improve the accuracy of dam site identification for flood risk reduction, outperforming traditional methods in precision and efficiency.

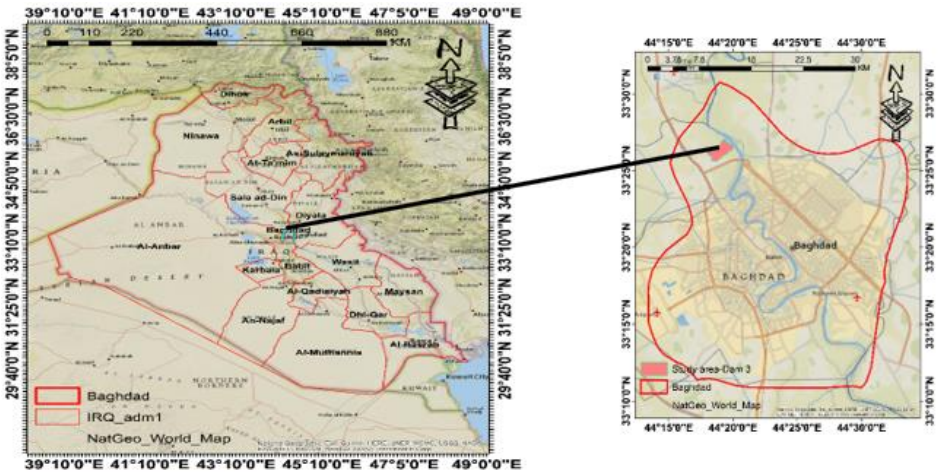

Figure (1): Study area, Baghdad City

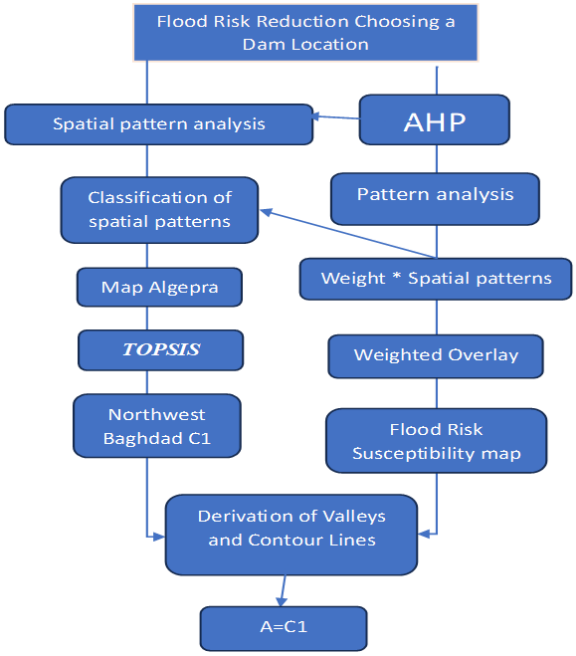

Figure 2. Flow chart showing the adopted methodology

Method Identifies Flood Areas

Remote sensing sensor data must cover red and infrared bands to analyze vegetation accurately. The NDVI, calculated from Landsat 8 images, helps identify flooded areas and soil stabilization effects. It ranges from 1 to -1, with 1 indicating high vegetation cover, acts as a natural filter, and the results show an estimate of 3% vegetation cover by Equation (1), as shown in Table (4,6) and Figure (3). Sensor data should capture NIR and SWIR bands for the Normalized Difference Water Index (NDBI). This index, derived from Landsat 8 images, identifies flood-prone areas affected by urbanization. Higher values indicate increased urbanization, Obtaining an urban area ratio of 17%, as shown in Equation (2), Table (4,6), and Figure (4).To assess water content using the Normalized Difference Water Index (NDWI), sensor data should include water, NIR, and green bands, NDWI values range from -1 to 1, aiding in dam site selection and flood risk evaluation, the result reveals that the proportion of wet soil areas was 9% as shown in Equation (3), As shown in Table (4,6), and Figure (5). The Normalized Difference Moisture Index (NDMI) requires soil index bands to calculate soil moisture content. NDMI values range from -1 to 1 and are crucial, for dam construction site identification. Wet soil areas account for 12%, as shown in Equation (4), As shown in Table (4,6), and Figure (6). This study highlights Baghdad's flood-prone nature and recommends building a dam in the northwestern city periphery. Quantitative results are derived from specific equations detailed in tables, with the Analytical Hierarchy Theory assisting in flood risk assessment.

$NDVI = \frac{NIR-R}{NIR+R}$... (1) $NDBI = \frac{NIR-SWIR}{NIR+SWIR}$ ... (2)

$NDWI = \frac{GREEN-NIR}{GREEN+NIR}$ ... (3) $NDMI = \frac{BAND5-BAND6}{BAND5+BAND6}$ ... (4) $TWI = \frac{ln\,(As)}{Tan}$ ... (5)

AHP Weight Extraction Method

The Analytical Hierarchy Process (AHP) is a decision-making method developed by Thomas Saaty in the 1980s. It provides a structured approach for comparing and prioritizing alternatives based on multiple criteria. AHP involves steps like goal setting, criteria analysis, alternative evaluation, and determining relative preferences. This method helps break down complex decisions into manageable parts, enabling informed decision-making. AHP finds applications in various fields such as engineering, project management, environmental sciences, and business economics, aiding in accurate decision outcomes.

$r_{ij} = \frac{x_{ij}}{\sum_{i=1}^{n} x_{ij}}$..... (6) $W_{ij} = \frac{\sum_{i=1}^{n} r_{ij}}{n}$ ..... (7) $v_{ij} = W_{ij} \times X_{ij}$ ..... (8)

$\gamma_{max} = \frac{\sum_{i=1}^{n} W_{ij} \times X_{ij}}{n}$ .....(9) $CI = \frac{(\gamma - n)}{n-1}$ .....(10)

The Analytic Hierarchy Process (AHP) is a precise and scientifically validated method for determining weights accurately. Crafted by experts, it ensures reliability and accuracy in decision-making. The empirical data and insights from specialists, as depicted in Table (1), are invaluable in this process.

Table (1): Decision maker table.

Order Matrix	1	2	3	4	5	6	7	8	9	10
RI	0.00	0.00	0.58	0.9	1.12	1.24	1.23	1.41	1.45	1.49

The study's variable weights were derived meticulously using the Analytic Hierarchy Process (AHP). Using the provided equations, weights for each pattern were determined and documented in Tables (2) and (3). These AHP-derived weights were seamlessly integrated with GIS, overlaying them onto pattern-specific maps. AHP offers a structured approach for extracting weights crucial in decision-making, enhancing the precision and effectiveness of the analytical framework.

TOPSIS Method

TOPSIS (Technique for Order Preference by Similarity to Ideal Solution) is a decision-making method developed by Hwang and Yoon in 1981. It aids in choosing the best option from a set of choices based on specific criteria. By assessing proximity to the ideal solution and distance from the worst solution, TOPSIS helps in evaluating alternatives. This method involves normalizing criteria values, assigning weights, identifying ideal and anti-ideal solutions, calculating similarity measures, and determining the relative closeness to the ideal solution for each alternative. Widely used in engineering, business, and environmental fields, TOPSIS assists decision-makers in selecting the most optimal alternative considering multiple criteria.

$\bar{X} = \frac{X_y}{\sqrt{\sum_{i=1}^{n} X_y^2}}$... (11) $V_{ij} = \overline{X_{ij}} \times W_j$ ... (12) $S_i^+ = \left[\sum_{j=1}^{m} \left(V_{ij} - V_j^+\right)^2\right]^{0.5}$ ... (13)

$S_i^- = \left[\sum_{j=1}^{m} \left(V_{ij} - V_j^-\right)^2\right]^{0.5}$ ... (14) $P_i = \frac{S_i^-}{S_i^+ + S_i^-}$ ... (15)

The methodology integrates the Analytical Hierarchy Process (AHP) with hierarchical chain theory to identify the prime dam construction location, considering factors represented in Table (2) with precise weightings in Table (3). AHP combined with GIS spatial configurations converts these weights into distances, further refined through the Technique for Order of Preference by Similarity to the Ideal Solution (TOPSIS). Spatial data from maps is weighted and aggregated, refined through TOPSIS as demonstrated in Table (6). Detailed analysis involves prescribed equations, vertical and horizontal summations, normalization, and multiplication by designated weights in Tables (7) and (8). Classification of geographical zones aids in pinpointing the optimal dam site, with region C1 ranking highest in Table (9) and achieving a suitability rating of 88.15% with a TOPSIS score of P=0.667, validating it as the best region for dam construction.

Table (2): Values of factors and optimal patterns developed by experts for decision-making in the Matrix.

rij	**Rain rate**	**Slop**	**River distance**	**Road distance**	**Urban distance**	**LULC 2022**	**NDVI**	**NDWI**	**NDMI**	**NDBI**
Rain rate	1	3	2	4	5	7	8	2	6	9
Slop	0.333	1	0.667	1.333	1.667	2.333	2.67	0.667	2	3

River distance	0.5	1.5	1	2	2.5	3.5	4	1	3	4.5
Road distance	0.25	0.75	0.5	1	1.25	1.75	2	0.5	1.5	2.25
Urban distance	0.2	0.6	0.4	0.8	1	1.4	1.6	0.4	1.2	1.8
LULC 2022	0.1428	0.5	0.333	0.666	0.833	1	1.14	0.29	1.2	1.8
NDVI	0.125	0.375	0.25	0.5	0.625	0.875	1	0.25	0.75	1.125
NDWI	2	0.67	1	0.5	0.4	0.29	0.25	1	3	4.5
NDMI	6	2	3	1.5	1.2	0.86	0.75	3	1	1.5
NDBI	9	3	4.5	2.25	1.8	1.3	1.13	4.5	1.5	1
sum	19.55	13.395	13.65	10.55	11.28	19.14	22.54	13.61	21.15	28.68

Table (3): Weight extraction using matrix normalization method.

Wij	**Rain rate**	**Slop**	**River distance**	**Road distance**	**Urban distance**	**LULC 2022**	**NDVI**	**NDWI**	**NDMI**	**NDBI**	**Weight**
Rain rate	0.05	0.23	0.147	0.38	0.3	0.37	0.35	0.15	0.28	0.34	0.26
Slop	0.017	0.075	0.049	0.126	0.15	0.122	0.12	0.049	0.095	0.1	0.09
River distance	0.026	0.11	0.073	0.19	0.22	0.183	0.18	0.073	0.14	0.16	0.12
Road distance	0.013	0.056	0.037	0.095	0.11	0.09	0.089	0.037	0.071	0.08	0.068
Urban distance	0.01	0.045	0.029	0.076	0.09	0.073	0.07	0.03	0.057	0.06	0.054
LULC 2022	0.007	0.037	0.024	0.063	0.074	0.052	0.05	0.02	0.057	0.06	0.044
NDVI	0.006	0.027	0.0183	0.047	0.055	0.046	0.044	0.018	0.035	0.039	0.034
NDWI	0.1	0.05	0.073	0.047	0.035	0.0152	0.011	0.073	0.14	0.16	0.084
NDMI	0.31	0.15	0.23	0.14	0.1	0.045	0.033	0.22	0.047	0.052	0.13
NDBI	0.46	0.224	0.33	0.21	0.16	0.068	0.05	0.33	0.07	0.035	0.19
SUM	1	1	1	1	1	1					1.074

Table (4): Weight normalization method

N W	**Weight (W)**	$\overline{\boldsymbol{Weight}\ (\overline{\boldsymbol{W}})}$	**Weight (%)**
Rin rate	0.26	0.24	24%
Slop	0.09	0.08	8%

River distance	0.12	0.11	11%
Road distance	0.068	0.07	7%
Urban distance	0.054	0.05	5%
LULC 2022	0.044	0.04	4%
NDVI	0.034	0.03	3%
NDWI	0.084	0.09	9%
NDMI	0.13	0.12	12%
NDBI	0.19	0.17	17%
SUM	1.074	1	100%

Table 5: Weighted sum vector and consistency vector

Rin rate	4.18	**17.42**
Slop	1.3934	**17.41**
River distance	2.09	**19**
Road distance	1.045	**14.92**
Urban distance	0.836	**16.72**
LULC 2022	**0.749542**	**17**
NDVI	**0.5225**	**17.42**
NDWI	**1.9327**	**21.47**
NDMI	**2.7969**	**23.31**
NDBI	**3.9834**	**23.43**

The average of the consistency vector (λ) is simply the arithmetic mean of the consistency vector from Table 4, and a sample calculation is included below. Equation (9) is used where n = 10 (since there are ten criteria) to determine C I, which indicates a high level of consistency since it is less than 0.1.

$$\lambda = \frac{17.42+17.41+19+14.92+16.72+17+21.47+23.31+23.43}{10} = 18.81$$

CI=0.0979

Table 6: *This table shows the numerical analysis and classification of 10 criteria. The weight is given to each criterion for the standardized vegetation index, the standardized urban area index, the standardized runoff difference index, and the moisture difference index. These results range from (1 to -1). If they are larger or smaller than this range, the results are incorrect. These results were calculated using the equations mentioned above and (1,2,3,4). Distance from the river Distance by distance from urban areas Land slopes and land uses and rainfall. It is possible to obtain the percentage of each criterion and its impact on floods through numerical analysis. Through these analyses, we can predict areas exposed to floods.*

Table 6

Flood causative criterion	Unit	Class	Susceptibility class Ranges and Ratings	Susceptibility Class Ratings	Weight (%)
NDVI	level	0.1514951 - 0.5088355 0.089796 - 0.1514951 0.0486633 - 0.089796 -0.0078942 –-0.0486633 -0.1467171- -0.0078942	Very High High Moderate Low Very Low	1 2 3 4 5	3%
NDBI	level	0.1666952 - 0.2920342 0.10972289 - 0.1666952 0.060347- 0.1097229 -0.16374396 -0.060347 -0.676493-- 0.16374396	Very High High Moderate Low Very Low	1 2 3 4 5	17%
NDWI	level	0.01931244 -0.5827558 0.04424885 - 0.0193124 0.083596 -0.04424885	Very High High Moderate	1 2 3	9%

		-0.13202398 -0.083596 -0.58906 - -0.13202398	Low Very Low	4 5	
NDMI	level	0.15614766 - 0.6764943 0.0641451 - 0.15614766 0.11352104 - 0.0641451 -0.1704933 -0.11352104 -0.292034 - -0.1704933	Very High High Moderate Low Very Low	1 2 3 4 5	12%
Road distance	level	3836.4 3836.4 – 7905.2 7905.2 – 11974.1 11974.1 – 16624.2 16624.2 – 29644.6	Very High High Moderate Low Very Low	1 2 3 4 5	7%
River distance	Level	1,852 1,852- 3,704 3,704- 5,557 5,557- 7,409 7,409- 9,261	Very High High Moderate Low Very Low	1 2 3 4 5	11%
LULC 2022	Level	Agriculture land Omran Vegetation Barren land water	Very High High Moderate Low Very Low	1 2 3 4 5	4%
Urban distance	Level	68248-155471 12694-27188 25959- 27147 27469- 12907 14248- 63882	Very High High Moderate Low Very Low	1 2 3 4 5	5%
Slop	Level	0.0145085 0.0145085 - 0.037722 0.037722 - 0.069641 0.069641 - 0.136379 0.136379 - 0.739931	Very High High Moderate Low Very Low	1 2 3 4 5	8%
Rin rate	Level	440.70 440.70 - 1,066 1,066- 1,691 1,691- 2,316 2,316- 2,942	Very High High Moderate Low Very Low	1 2 3 4 5	26%
					100

Table (7): Data matrix for the selected regions for each factor.

r	Rain rate	Slop	River distance	Road distance	Urban distance	LULC2022
C1	11.665	3	1468.8	4	2399.3	4
C2	7.757	2	2593.27	5	2647.4	2
C3	5.723	1	3353.6	5	3528.7	5
C4	1.745	1	6442.98	5	3972.8	7
$\sqrt{\sum_{i=1}^{n} X_y^2}$	19.233	3.87	7842.77	9.54	6396.94	9.695

Table (8): Normalizing data for specific regions.

$\bar{X}$	Rain rate	Slop	River distance	Road distance	Urban distance	LULC2022
C1	0.61	0.78	0.187	0.419	0.375	0.413
C2	0.403	0.52	0.331	0.524	0.414	0.21
C3	0.26	0.26	0.428	0.524	0.552	0.516
C4	0.09	0.26	0.822	0.524	0.621	0.722
Weight	0.26	0.08	0.11	0.07	0.05	0.04

Table (9): Multiplying the data by its weights and extracting (V+) and (V-)

Vij	Rain rate	Slop	River distance	Road distance	Urban distance	LULC2022
C1	0.16	0.062	0.021	0.0293	0.019	0.017
C2	0.11	0.042	0.036	0.037	0.021	0.0084
C3	0.068	0.021	0.047	0.037	0.028	0.0206
C4	0.0234	0.021	0.09	0.037	0.031	0.029
V^+	0.16	0.062	0.09	0.037	0.031	0.029
V^-	0.0234	0.021	0.021	0.0293	0.019	0.0084

Table (10): (P) is extracted and the highest number takes the rank (1), which represents the first region.

Ra	S_i^+	S_i^-	P_i	Rank
C1	0.0715	0.143	0.667	**1**
C2	0.088	0.091	0.508	**3**
C3	0.104	0.0544	0.344	**4**
C4	0.071	0.0734	0.509	**2**

Flood Risk Susceptibility map

The flood susceptibility map was created by categorizing criteria values into four groups and combining them to form a comprehensive map. Sub-criteria under each primary criterion were utilized in developing the final flood zoning map. Through AHP, the relative importance of each criterion was determined, with comparison matrices used to assign classification scores. By calculating the weighted sum of all causal factors, the final flood Susceptibility map was produced, and validated by a CR value of 0.0979 (<0.1). The NDWI criterion held significant influence with a weight of 0.09, followed by NDMI at 0.12. NDVI was assigned a weight of 0.03, and NDBI received 0.17. Other criteria such as rainfall (0.24), slope (0.08), distance from the river (0.11), distance from road (0.07), distance from urban areas (0.05), and land use/land cover (0.04) were also considered in the analysis (Table (5,6) and Figure 10).

CHOOSING THE APPROPRIATE PLACE TO BUILD THE DAM

ANALYSIS, CLASSIFICATION, AND INTEGRATION OF SPATIAL PATTERNS

Selecting a dam site to mitigate flood risks involves evaluating geographic factors like slopes (Figure 7-a), nearby rivers, and valleys. Data analysis, including past flood records and future projections, is crucial for understanding flood impacts. The distance between a river and a dam affects water flow dynamics and reservoir capacity, impacting dam placement and water storage (Figure 7-b). Rainfall patterns play a key role in site selection, influencing water availability and flow regulation in (Fig. 8-a). Analyzing land cover changes aids in identifying suitable dam locations by assessing runoff and water storage capacity maintenance (Figure 8-b). inning distance between roads and dams is vital for flood risk reduction, requiring proper planning and management, (Figure 9-a). Urban areas near dam sites pose challenges, impacting site selection and water quality. Integrating urban considerations with decision-making tools like AHP enhances flood risk management strategies effectively, As in (Figure 9-b).

AHP INTEGRATION WITH GIS AND THEN INTEGRATION WITH TOPSIS

A rigorous scientific methodology was utilized to determine the optimal dam construction site. The Analytical Hierarchy Process (AHP) was employed to derive precise weights, integrated with GIS for spatial analysis. The process categorized regions (C1, C2, C3, C4) and utilized the Technique for Order of Preference by Similarity to the Ideal Solution (TOPSIS) method. Region C1 emerged as the top choice, scoring 0.667 and surpassing others by 88.15%. This approach ensures accuracy and precision in selecting the most suitable dam location. See Figure (10) for visual representation.

DERIVATION OF VALLEYS AND DRAWING CONTOUR LINES

Valley passes are crucial for selecting the best reservoir location to optimize water retention while minimizing costs. Exploration identifies Wadi Al-Azim in Baghdad's northeast as a potential site with a capacity of 22,187,226.233 cubic meters. A less populated area northwest of Baghdad, owned by the state, is preferred for its suitability and no need for land acquisition. Detailed analyses of valleys and contour lines pinpoint the ideal dam location with a projected capacity of 31 million cubic meters, significantly reducing flood risks in Baghdad (see Fig 11-a). Contour lines are vital in site assessment, with closely spaced lines indicating prime locations for efficient water retention. Managing the spacing between contour lines is critical for cost-effective dam construction. Careful examination of contour lines helps determine the optimal dam length, (see Fig 11-b).

EVALUATING DAM LOCATIONS THROUGH VALLEY DERIVATION AND CONTOUR ANALYSIS"

Three potential dam sites in Baghdad were evaluated: Dam A (northwest), Dam B (southwest), and Dam C (northeast). Dam B was rejected due to being in a residential area. Dam A was chosen for its water sources and topographical advantages, with a capacity of 31 million cubic meters. Dams B and C had smaller capacities and higher population densities. The decision was based on land ownership, population density, and site condition, using valley derivation techniques and the TOPSIS method. Figures (12), and (13) illustrate the selection process for Dam A.

TOPSIS INTEGRATION WITH THE DERIVATION OF VALLEYS AND CONTOUR LINESREFERENCES

Valley and contour lines integration with the TOPSIS method is crucial for dam site evaluation. Dam A (31 million cubic meters) was selected over Dam C (22,187,226.23 cubic meters) due to cost, size, and population factors. Pixel processing determined Dam A's capacity at 28,177,200 cubic meters, surpassing 50% of the main basin volume, while Dam C's capacity was 21,654,000 million *cubic meters. The selection of Area C1 (C1=A) outside Baghdad city is justified by state ownership and low population density. Figures (14 A, C), (15, A, C), and Table 11 offer visual insights.*

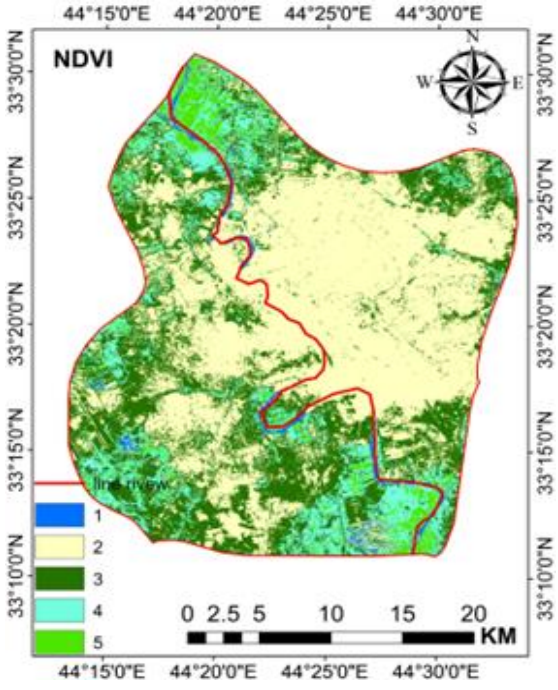

Figure (3): represents the vegetation area index.

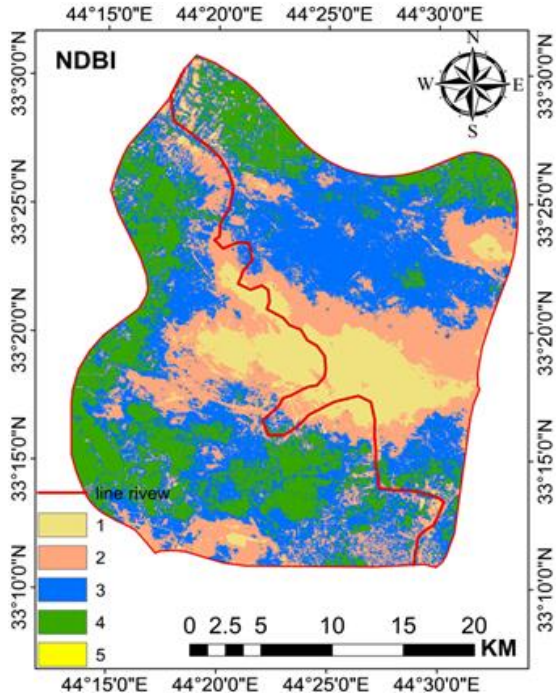

Figure (4): represents the urban areas index.

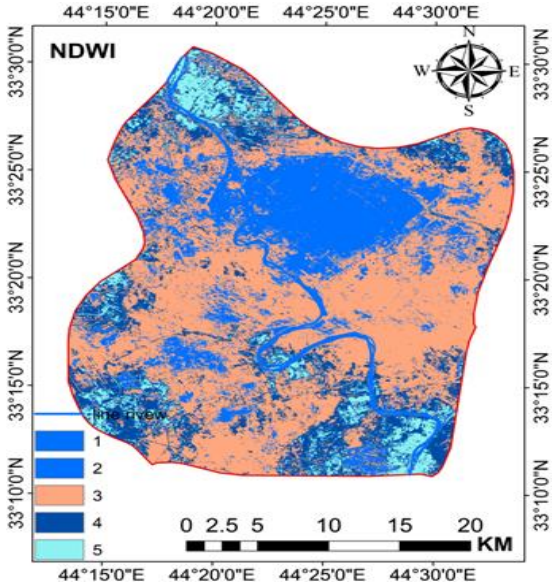

Figure (5): Difference Water Index (NDWI).

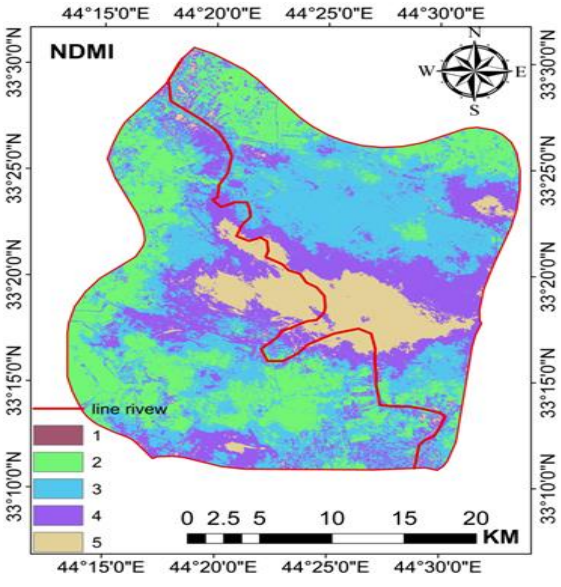

Figure (6). Soil moisture difference index.

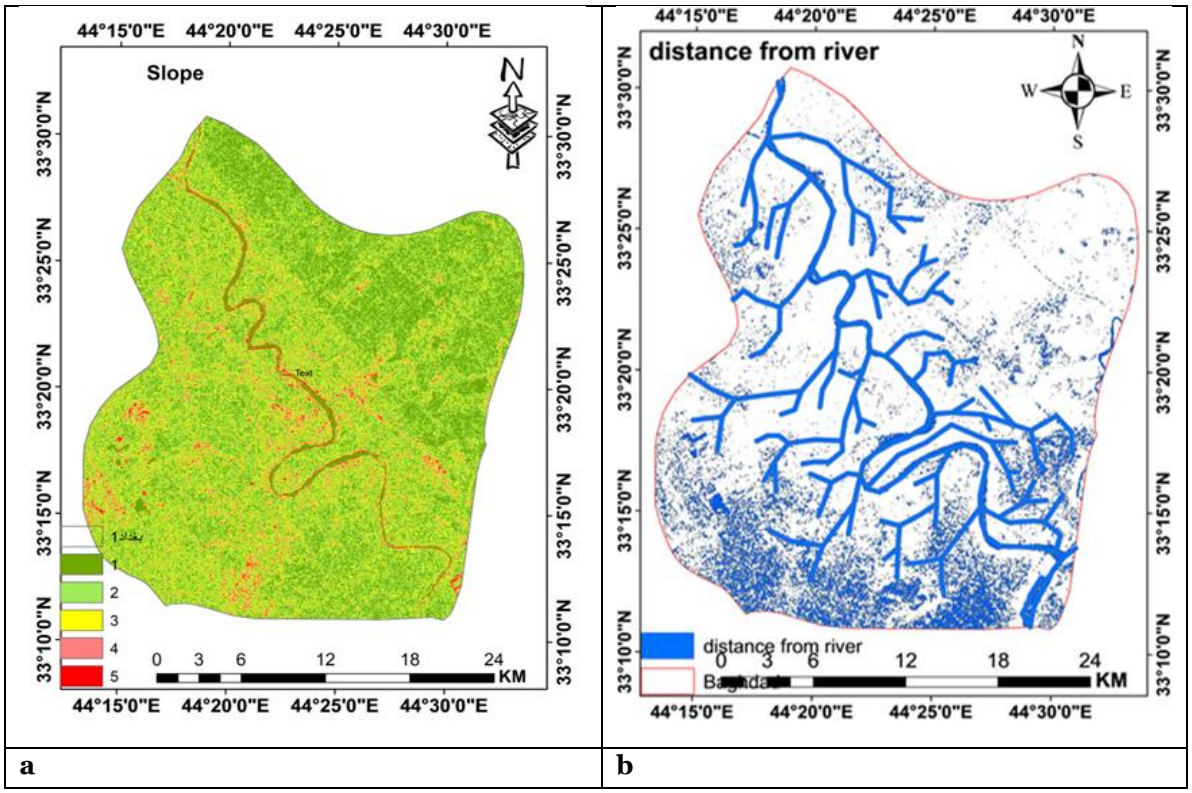

Figure 7 represents the slope of the land (a), after the dam from the river (b).

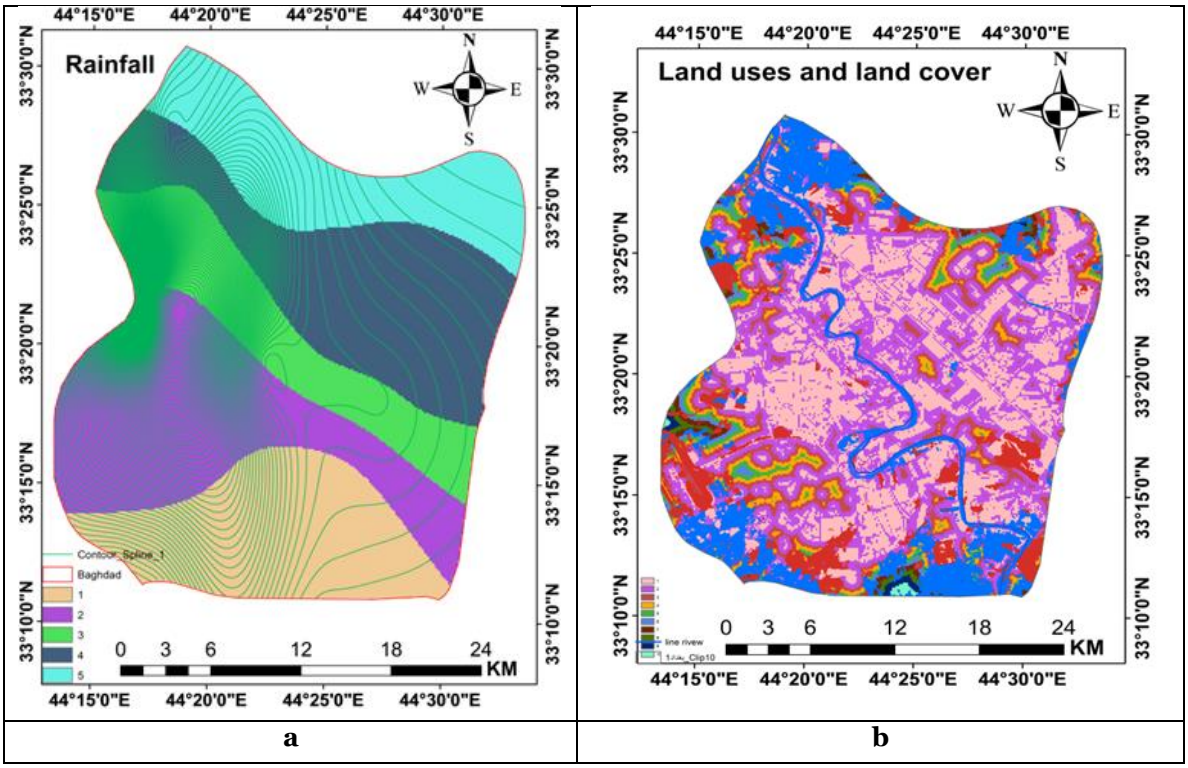

Figure 8: represents the rain analysis (a) and the land use analysis (b)

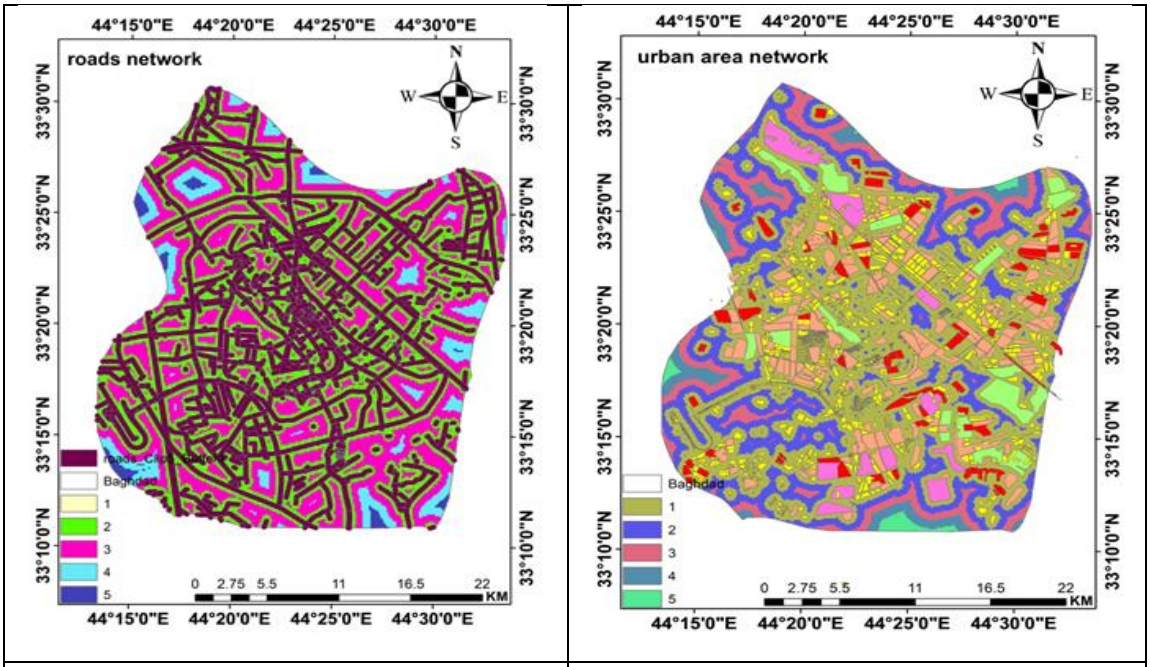

a b

Figure 9: The distance of the road from the dam (a), the impact on urban areas (b).

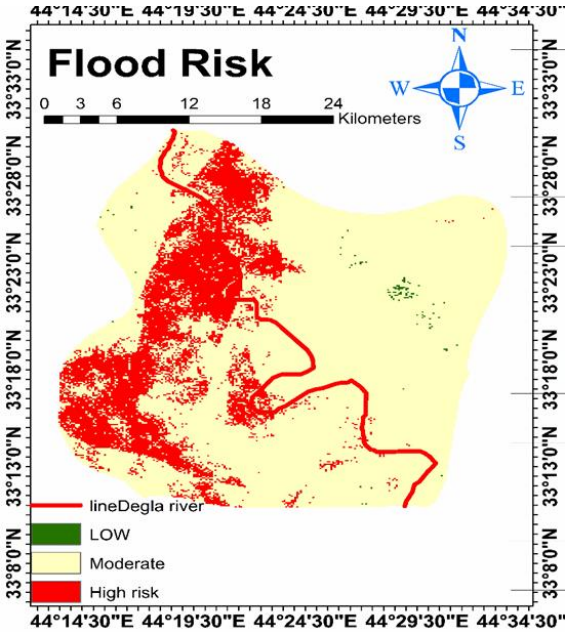

Figure (10): Determining the flood areas. notice that obtained from this result, this Figure, that the flood areas are more a risk in the northern and northwestern regions. This result could determine the dam's location.

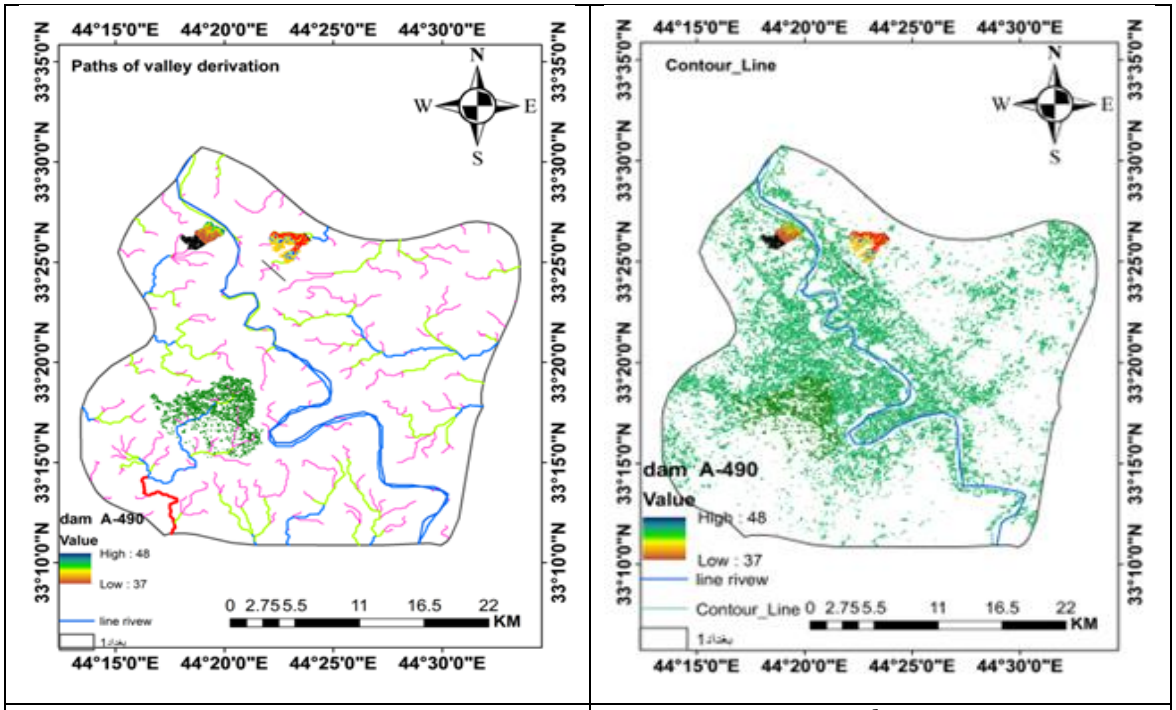

a b

Figure (11): which represents the paths of valley derivations (a) and contour lines (b)

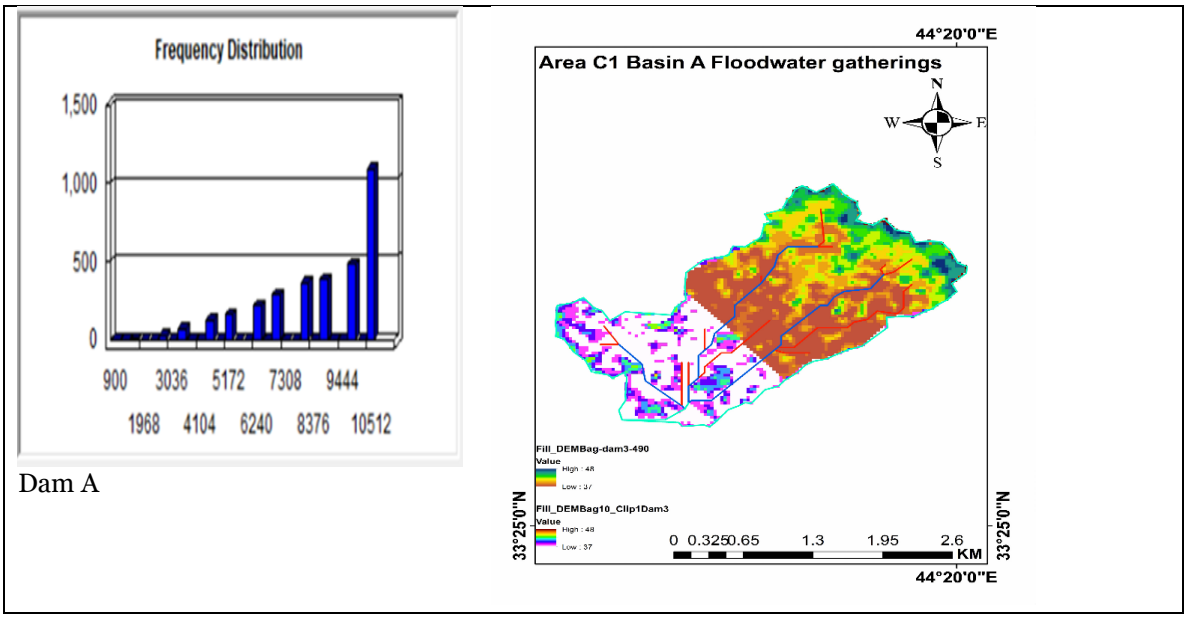

Figure (12): Northwest Baghdad Dam and size chart of Northwest Baghdad Dam

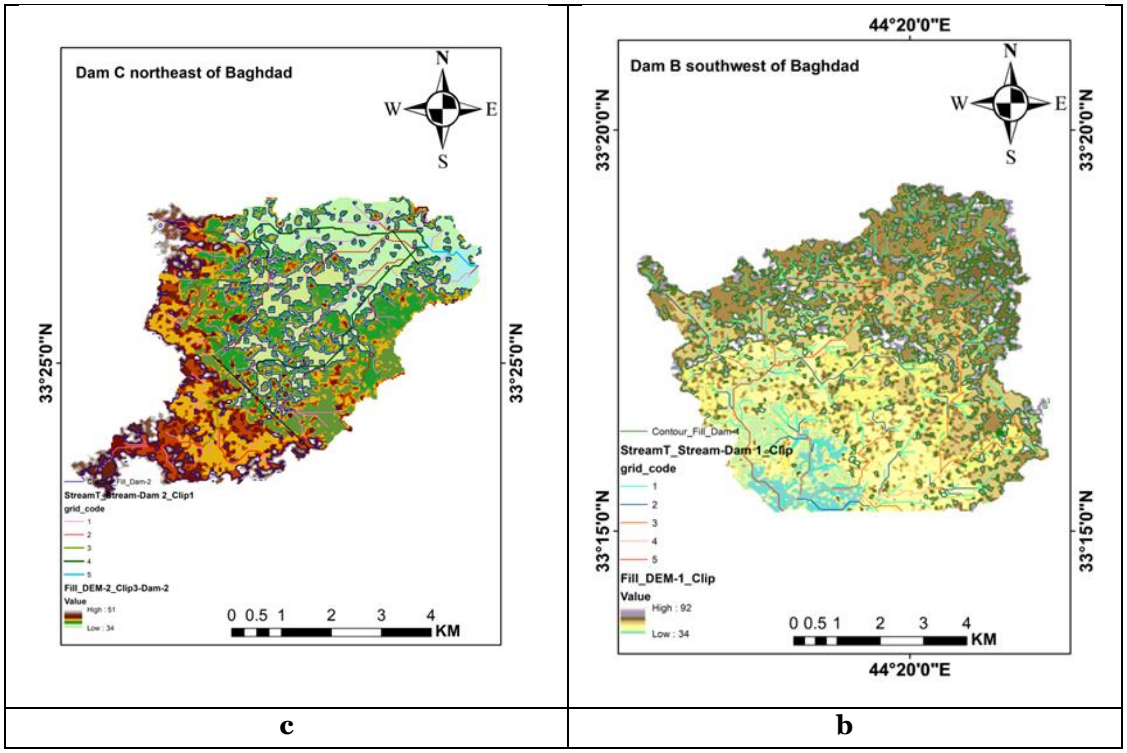

c **b**

Figure (13): Northeast Baghdad Dam (c), Southwest Baghdad Dam (b).

Table 11 displays the dam basin areas in different regions: northwest of Baghdad (a), southwest of Baghdad (b), and northeast of Baghdad (c). While the areas of these basins are approximately equal, there are variations in rainfall. As move north, the rainfall rate increases, resulting in differences in water absorption capacity across the basins. The pixel areas in the sub-basins (A, B, C) remain consistent, but the contour height varies, leading to differences in depth and water absorption volume among the basins.

Table 11: The dam basin areas in different regions.

r	Area (m2)	Depth	Pixel area	Rin-rate	Volume	Capacity
Dam -A	775000	40	900	0.7	31,000,000 m³	A=28,177,200 m³
Dam-B	443,245.25	40	900	0.4	17,729,810 m³	B=13,627,000 m³
Dam-C	554,680.656	40	900	0.5	22,187,226.23 m³	C=21,654,000 m³

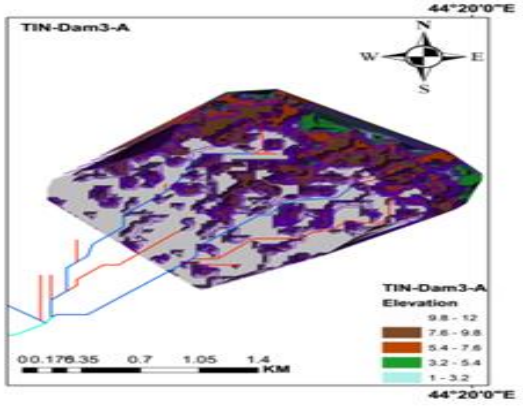

A

Figure (14): which includes the chosen Capacity Dam to the water basin (A)

C

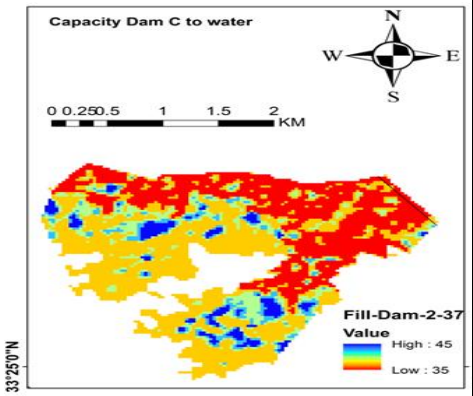

Figure (14): which includes the chosen Capacity Dam basin (C)

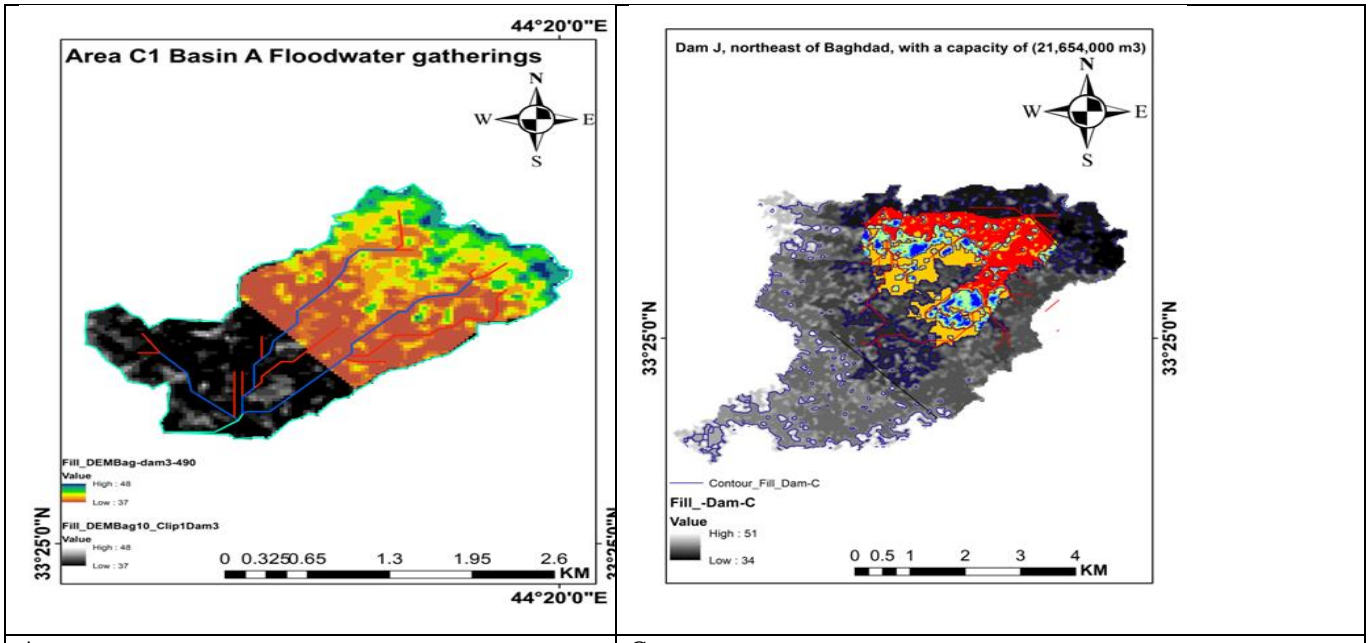

A C

Figure (15): The dam basin area northwest of Baghdad (A) and the dam basin area northeast of Baghdad (C).

Compare Results

- Regional Focus: This research is unique as it focuses on Baghdad, Iraq, an underrepresented region in flood mitigation research. Previous studies have concentrated on areas like Iran (Jozaghi et al.), India (Pathan et al.), and Turkey (Karakuş et al.), with a limited focus on the Middle East.
- Data Inputs: The study incorporates flood inventory datasets and integrates climate change considerations into the analysis (e.g., rainfall patterns, land use, proximity to water bodies, terrain slopes). Many similar studies lack such emphasis on long-term climate variability.
- Outputs: work identified the best dam site (C1 = Dam A), achieving a suitability score of 0.667 and demonstrating 88.15% completion efficiency. These findings contrast with studies like those of Jozaghi et al., who often compare methods without definitive site recommendations.
- "Our research addresses gaps in the literature by focusing on Baghdad, a region with limited prior studies on flood mitigation through dam site selection. In contrast to studies by Jozaghi et al. (2018) and Pathan et al. (2022), which concentrate on comparative methodologies, we provide actionable results by identifying the most suitable site with a suitability score of 0.667 and an 88.15% completion efficiency. Additionally, this study uniquely incorporates climate change considerations, enhancing the robustness and applicability of the results to dynamic environmental conditions."
- "This research builds on prior studies that integrate GIS with multi-criteria decision-making approaches. Jozaghi et al. (2018) and Pathan et al. (2022) demonstrate the utility of AHP and TOPSIS in dam site selection; however, their focus remains limited to specific regions and lacks the integration of advanced hydrological analyses like valley derivation and contour mapping. By situating this study in Baghdad and addressing long-term climate variability, we extend the applicability and robustness of these methodologies."

Discussion of Results

After analyzing various metrics, flood-prone areas were pinpointed. The standardized indices for water, humidity, vegetation, and urban areas were 9%, 12%, 3%, and 17% respectively. Factors like distance from roads, rivers, land slope, land use, rainfall, and population density also played a role. The Analytical Hierarchy Process (AHP) translated these weights into distances using map data, aiding in the identification of flood-prone areas within Baghdad. The TOPSIS technique further refined this analysis, highlighting Area C1 as the optimal dam site with an 88.15% agreement. Dam A in C1 boasts a basin volume of 31 million cubic meters, a water capacity of 28,177,200 cubic meters, and an area of 775 thousand square meters. The superiority of C1 in both TOPSIS and detailed analysis confirms its suitability for Dam A, affirming the accuracy of the findings.

Conclusions

The research paper focuses on flood risk mitigation through a detailed analysis of flood susceptibility using 10 criteria, including various indices such as NDMI, NDWI, NDBI, and NDVI, alongside factors like distance from rivers, roads,

land slope, land use, population density, and rainfall. Utilizing the Analytical Hierarchy Process (AHP) in Geographic Information Systems (GIS), subjective weights are standardized for comparison, and objective weights are derived from end-user ratings. A convergence coefficient aids in ranking alternatives based on distances to ideal and negative ideal solutions. The TOPSIS method aligns weights from critical factors, selecting the optimal region (C1) with a score of 0.667, indicating 88.15% suitability. By employing valley derivation and contour analysis, the dam location in region C1, situated between Baghdad and Salah al-Din, is precisely determined. Factors like size, capacity, area, and rainfall are crucial in screening dam sites. Integration with the TOPSIS method ensures accurate results, such as Dam A with a volume of 31 cubic kilometers and a capacity of 28,177,200 cubic meters.

REFERENCES

[1] Al-Ansari, N. (2014). Management of Water Resources in Iraq: Perspectives and Prognoses.
[2] Mourad, K. (2023). Climate Change and Water Scarcity in the Middle East: Challenges and Solutions.
[3] Eklund, L., Darcy. (2023). Infrastructure Vulnerabilities in the Middle East: The Case of Mosul Dam.
[4] Zahraa Al-Ali a, Ammar Abulibdeh b, Talal Al-Awadhi c d, Midhun Mohan e f, Noura Al Nasiri c, Mohammed Al-Barwani, Sara Al Nabbi c, Meshal Abdullah a c g, to detect soil moisture and flooded areas, https://doi.org/10.1016/j.jag.2024.103887
[5] Istak Ahmed, Nibedita Das, Jatan Debnath, Moujuri Bhowmik, Shaswati Bhattacharjee, https://www.sciencedirect.com/journal/geosystems-and-geoenvironment https://doi.org/10.1016/j.geogeo.2023.100250
[6] Huali Chen, Yuka Ito, Marie Sawamukai & Tomochika Tokunaga, a framework to map flood, https://link.springer.com/journal/11069
[7] Anne Gacul, Dexter Ferrancullo, Romel Gallano, KC Jane Fadriquela, Kyla Jane Mendez, John Rommel Morada, John Kevin Morgado, and Jerome Gacu, establish flood mitigation programs. http://dx.doi.org/10.32604/RIG.2024.055085
[8] Ahmed MA, Mohamed MH, Parvin MM, Ilić P (2022) The recurrence of natural disasters in Jowhar, Middle Shabelle Region, Somalia: the Causes and Impacts. J Environ Prot 13(9):657– 670. https://doi.org/10.4236/jep.2022.139042
[9] Rajib Mitra, Saha P, Das J (2022) Assessment of the performance of GIS-based analytical hierarchical process (AHP) approach for flood modeling in Uttar Dinajpur district of West Bengal, India. Geomatics. Nat Hazards Risk 13(1):2183–2226. https://doi.org/10.1080/19475705.2022.2112094
[10] Abdelhafid El Alaoui El Fels, Noureddine Alaa, Ali Bachnou, Said Rachidi, https://doi.org/10.1016/j.jafrearsci.2018.02.004, https://www.sciencedirect.com/journal/journal-of-african-earth-sciences
[11] 11. Liu C, Guo L, Ye L, Zhang S, Zhao Y, Song T (2021) A review of advances in China's flash flood early-warning system. Nat Hazards 92(2):619–634. https://doi.org/10.1007/s11069-018-3173-7
[12] Luca Pulvirenti, Marco Chini, and Nazzareno Pierdicca, InSAR Multitemporal Data over Persistent Scatterers to Detect Floodwater in Urban Areas, https://doi.org/10.3390/rs13010037
[13] Rizwan Sadiq, Zainab Akhtar, Muhammad Imran, Ferda Ofli, Integrating remote sensing and social sensing for flood mapping, https://doi.org/10.1016/j.rsase.2022.100697
[14] Andi Ridwan Makkulawu, Soemarno, Imam Santoso, Siti Asmaul Mustaniroh, Potential and Benefits of AHP and GIS Integration for Decision-Making DOI:10.18280/isi.280629
[15] 15. Nitin Liladhar Rane, Suraj Kumar Mallick, Anand Achari, Saurabh Purushottam Choudhary, Chaitanya B. Pande, Aman Srivastava, Kanak N. Moharir, for potential dam site selection using GIS, MIF and TOPSIS, https://doi.org/10.1016/j.jclepro.2023.138890
[16] Awadh, S. M. (2024). Drought and Desertification Hazard in Iraq. Springer. *Link*
[17] Muslih, K. D., & Abbas, A. M. (2024). Climate of Iraq. Springer. *Link*
[18] Al-Khalidi, J., Bakr, D., & Sedeeq, R. (2024). 850 hPa Geopotential Height Link with Iraqi Precipitation and Temperature. SciELO. Link
[19] Nassif, W. G., Al-Ataby, I. K., & Al-Taai, O. T. (2024). Impact of Soil Temperature and Precipitation on Vegetation Cover Over Selected Stations in Iraq. Asian Journal of Water, Environment and Pollution
[20] Alrawi, I., et al. (2021). Applications of Geographic Information Systems for Flood Risk Mitigation in Semi-Arid Regions. *Link*
[21] Mahdi, H. H. (2020). Flood Risk Assessment and Urban Resilience: A Case Study in Iraq. Scientific Journal of King Faisal University.
[22] Al-Hussein, A. A. M. (2024). Hydrological and Socioeconomic Impacts of Flood Events in Baghdad. ResearchGate.
[23] Jozaghi, A., Alizadeh, B., Hatami, M., Flood, I., Khorrami, M., Khodaei, N., & Ghasemi Tousi, E. (2018). A comparative study of the AHP and TOPSIS techniques for dam site selection using GIS: A case study of Sistan and Baluchestan Province, Iran. Geosciences, 8(12), 494.

[24] Pathan, A. I., Agnihotri, P. G., & Patel, D. (2022). Integrated approach of AHP and TOPSIS (MCDM) techniques with GIS for dam site suitability mapping: A case study of Navsari City, Gujarat, India. Environmental Earth Sciences, 81, 443.
[25] Ali Jozaghi, Babak Alizadeh, Mohsen Hatami, Mohammad Khorrami, Nastaran Khodaei. A Comparative Study of the AHP and TOPSIS Techniques for Dam Site. https://doi.org/10.3390/geosciences8120494
[26] Azaz Khan Ibrahim Khan Pathan, Prasit Girish Agnihotri & Dhruvesh Patel, (2022): Integrated AHP and TOPSIS approach for dam site mapping in Gujarat, India (Springer).
[27] C. B. Karakuş & S. Yıldız. (2022): GIS-based AHP for land suitability assessment in Turkey (Springer)
[28] Abbas Mohammed Noori, Biswajeet Pradhan, Qayssar Mahmood Ajaj Dam site suitability assessment at the Greater https://doi.org/10.1016/j.jhydrol.2019.05.001
[29] Junwei, Ma & Ali Mostafavi, spatial inequality of property flood risk, https://doi.org/10.1038/s43247-024-01337-3